Int. J. Electrochem. Sci., 10 **(2015)** 7771 - 7782

International Journal of
ELECTROCHEMICAL
SCIENCE
www.electrochemsci.org

Electron Beam Irradiated ZnO Nanoparticles / Oxidized MWCNTs Modified GCE as a Supercapacitor

Deepu Thomas[1,2,*], *Tony Thomas*[3,*], *Jithin Prakash P A*[4], *Tomlal Jose E*[5] *and Simon Augustine*[2]

[1]Research and Development Centre, Bharathiar University, Coimbatore 641046, India.
[2]Research and Post-Graduate Department of Physics, St.Thomas College, Pala, Kottayam 686574, India.
[3]Department of Chemistry, Deva Matha College, Kuravilangad, Kottayam 686633, India.
[4]Research and Post-Graduate Department of Chemistry, St.Thomas College, Pala, Kottayam 686574, India.
[5]Research and Post-Graduate Department of Chemistry, St. Berchmans College, Changanassery, Kottayam, 686 101, India.
[*]E-mail: deepuskariankal@gmail.com; tonytk201@gmail.com

Received: 2 June 2015 / *Accepted:* 11 July 2015 / *Published:* 28 July 2015

A supercapacitor with promising features has been developed by modifying glassy carbon electrode (GCE) with electron beam irradiated ZnO nanoparticles (NPs) and oxidized MWCNTs ($MWCNTs_{OX}$). ZnO NPs of spherical shape was synthesized by sonochemical method. Various quantities of oxidized MWCNTs have been added to improve the specific capacitance of ZnO NPs modified GCE. 1:5 ratio of ZnO NPs and oxidized MWCNTs provides the maximum specific capacitance. The proposed method of electrode fabrication enables us to get the desired specific capacitance values by carefully controlling the ratios of ZnO NPs and oxidized MWCNTs. Surface morphologies of the electrodes have been analyzed by SEM and found that electrode surfaces are uniformly coated with ZnO NPs and oxidized MWCNTs. A specific capacitance of 372 Fg^{-1} was obtained for present electrode which is highest among similar electrodes. Synergetic effect of irradiated ZnO NPs and oxidized MWCNTs is responsible for unusual enhancement in capacitance. The proposed electrode is found to be easy to prepare, environmentally benign, stable and economic.

Keywords: ZnO NPs, oxidized MWCNTs, Synergism, Supercapacitor, Environmentally benign

1. INTRODUCTION

The growing energy demands of modern society forced human beings to develop some excellent energy systems for storage and conversion. Thus, the designing of simple electrochemical

capacitors has attracted many [1-4]. Electrochemical capacitors find the gap between batteries and conventional capacitors such as electrolytic capacitors or metalized film capacitors in terms of specific energy and specific power which raised the attraction for the development of supercapacitors [5-11]. Moreover, electrochemical capacitors are promising materials for energy storage because of high power capability, fast charge/discharge rates, long cycle life, and low maintenance cost [5].

Construction of electrochemical capacitors using carbonaceous materials such as carbon nanotubes (CNTs), activated carbon, carbon onions, carbon fibers and graphene is well reported [12-18]. CNTs are proved to be worth materials in various fields of science and technology, since their discovery in 1991 by Iijima. CNTs have excellent electronic conductivity, thermal and chemical stability, ultra-light weight and high surface area [19]. CNTs can be mainly divided into single-walled carbon nanotubes (SWCNTs) and multi-walled carbon nanotubes (MWCNTs) [20-22]. CNTs based composite electrodes have been extensively used in the fabrication of electrochemical capacitors. CNTs play as perfect super capacitors in combination with conducting polymers and metal oxides [22]. Small quantities of MWCNTs are large enough to improve the performance of the electrode.

Among the various metal oxide nanoparticles(NPs), ZnO as an important semi conducting material has a lot of applications in optics, optoelectronics and sensors [23-36]. Selvakumar et al. reported that ZnO is a well-known battery active material having high energy density of 650 A/g [27]. ZnO NPs are good materials for vast applications in various fields because of low cost as a raw material, good electrochemical activity and environmentally friendliness compared with other metal oxides. However, low rate of power capability and poor recyclable capability during cycling make ZnO NPs inappropriate for supercapacitor applications. Substantial efforts have been devoted to surmount these problems by fabricating composites with materials such as MWCNTs. Moreover, conductance of ZnO NPs could be improved by irradiating it with electron beams. Pseudo capacitance of ZnO NPs and double layer capacitance of MWCNTs offers an elevation in specific capacitance. MWCNTs act as good supporting material for ZnO NPs and together form a supercapacitor of enhanced performance.

Considerable amount of research has been devoted to fabricate supercapacitors of high power capability for various energy needs. In the present work, our objective was to develop simple, efficient and cost effective super capacitor by combining the properties of electron beam irradiated ZnO NPs and oxidized MWCNTs. It was successfully demonstrated in the present study that addition of $MWCNTs_{OX}$ to ZnO NPs generates greater specific capacitance at an optimized ratio and which has not yet been reported elsewhere unto the best knowledge of authors.

2. EXPERIMENTAL

2.1 Reagents

Zinc sulfate heptahydrate **(**$ZnSO_4.7H_2O$), Acetic acid (CH_3COOH), Sodium dodecyl sulfate (SDS), Sodium hydroxide(NaOH) pellets, ethanol (C_2H_5OH), Nitric acid (HNO_3) and Potassium hydroxide(KOH) were purchased from Merck. MWNTs (6–20 nm diameter and 1–5 mm length) and Nafion were purchased from Aldrich. The chemicals employed in this experiment were of AR grade

quality and they were used without further purification and all the aqueous solutions were prepared with ultra pure water (<18.2MΩ cm) from Milli-Q-Plus system (Millipore).

2.2 Instrumentation

The optical absorption of the ZnO NPs was recorded with a Perkin–Elmer Lambda 35 UV–Visible spectrometer. The surface morphology and structure of the samples were characterized by scanning electron microscopy (SEM, Philips XL 30), transmission electron microscope (TEM, JEM 3010) operated at 200 kV, and X-ray diffraction spectroscopy (XRD, PTS 3003) with Cu Kα radiation (λ = 1.5418 Å).

An electron beam of 8 MeV energy is obtained from the Microtron, Department of Studies in Physics, Mangalore University, Mangalagangotri was used for irradiation of ZnO particles. Specifications of electron beam used for irradiation are as follows: beam energy: 8 MeV, beam current: 25–30 mA, beam size: 5 mm × 5 mm, pulse repetition. Rate: 50 Hz, pulse width: 2.5 μs, dose rate: 8 kGy/min (Fricke dosimetry). The sample was kept at a distance of 30 cm from the target.

Cyclic voltametric studies were carried out with an electrochemical analyzer (BAS Epsilon Bioanalytical System, USA) coupled to a PC. The voltammetry was performed using a glassy carbon and modified glassy carbon electrodes were used as working electrode, Ag/AgCl as reference electrode and Pt wire as auxiliary electrode. All cyclic voltammetric measurements were performed with a scan rate of 100 mV s^{-1}.

2.3 Preparation of ZnO nanoparticles and its electron irradiation

The ZnO nanoparticles were prepared by the modification of method reported elsewhere [37, 38]. In a typical experiment, first solution was prepared by dissolving 8.636 g $ZnSO_4$. 3.603 ml CH_3COOH and 40 mg SDS as surfactant in 1 dm^3 of water. The second solution was prepared by 3.6 g NaOH pellets and 25 ml 70% of ethanol. Then the first solution was slowly added to the second solution with continuous stirring. The mixture was sonicated (20 kHz, 350 W) and then microwave irradiated (20% power for 20 minutes, 700watts) to avoid agglomeration. The obtained precipitate was filtered using a Whatmann filter (grade-41) and the sample was air dried. The white solid product was then washed with ethanol and water to remove impurities. The dried precipitate was calcinated at 550^0 C for one hour to form ZnO nanoparticles. The prepared ZnO nanoparticles were irradiated with electrons at a dose of 8 kGy at room temperature.

2.4 Acid treatment of pristine MWCNTs (pMWCNTs)

Acid treatment of pMWCNTs was carried out as reported elsewhere [39]. pMWCNTs were refluxed in 100 ml 6 M HNO_3 for 10 h. The resulting suspension was then diluted with 200 ml of water, filtered and washed with double distilled water. The washed nanotubes were collected and dried. The acid treated pMWCNTs were designated as oxidized MWCNTs ($MWCNTs_{OX}$). The acid

treatment eliminates the metal oxide impurities in pMWCNTs and introduces oxygen functionalities at the ends of pMWCNTs and along the tube. The acid treatment also results in shortening of pMWCNTs which in turn helps in better dispersion.

2.5. Preparation of ZnO-MWCNTs$_{OX}$-modified GCE.

The GCE was mechanically polished with alumina slurry down to 0.05 mm on a polishing cloth, prior to modification. GCE was then sonicated in methanol, water, HNO_3 solution and acetone, respectively. 5.012 mg of MWCNTs$_{OX}$ was dispersed in 2 ml of 0.5 % Nafion–water solution with the aid of ultrasonic agitation to form a black homogeneous suspension. 4 μL of dark suspension was drop cast onto the surface of GCE. The electrode was then allowed to dry in air to obtain the MWCNTs$_{OX}$-modified GCE (GCE/ MWCNTs$_{OX}$).

5.031 mg of ZnO was dispersed in 2.0 ml of 0.5 % Nafion-water solution under ultrasonication. Various quantities (1.0 ─ 3.0 μL) of this solution was cast on a clean GCE and dried. The prepared electrode was abbreviated as GCE/ZnO. A mixture containing 1:1, 1:3 and 1:5 compositions of ZnO and MWCNTs$_{OX}$ were cast on the surface of GCE. The prepared electrodes are termed as GCE/ZnO/MWCNTs$_{OX}$.

3. RESULTS AND DISCUSSION

3.1 XRD studies

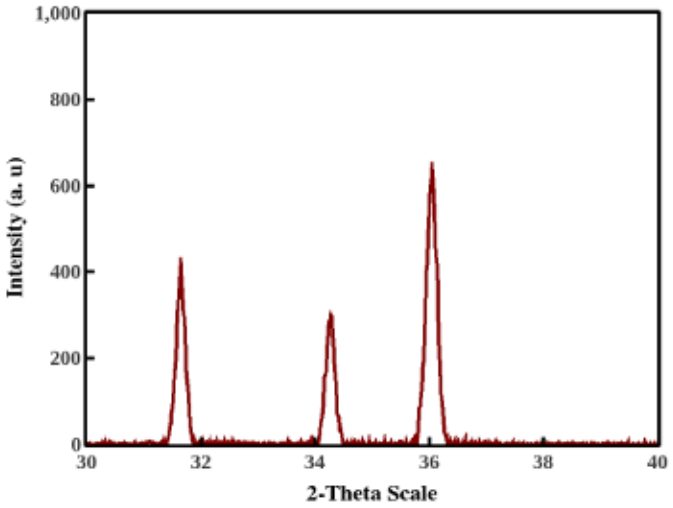

Figure 1. XRD patterns of ZnO NPs.

Fig. 1 shows PXRD patterns of nano ZnO crystals. The broadening in the XRD peaks reveals the nanocrystalline nature of the particles. The particle size was calculated using the Scherer equation and was found to be 44 nm. PXRD pattern shows a maximum intense peak at 36.2° and the corresponding value was found to be 2.481 Å which indicates hexagonal crystal structure of ZnO [37].

3.2 UV-Visible Spectroscopy

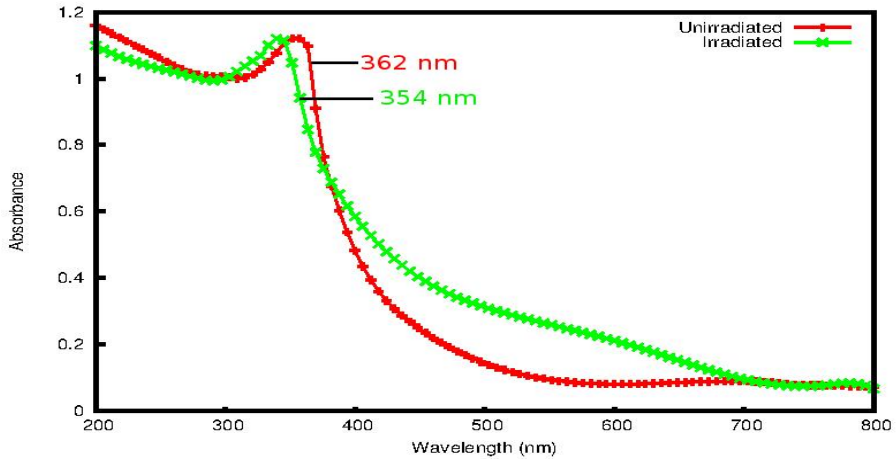

Figure 2. UV- spectra of unirradiated and irradiated ZnO NPs.

Fig. 2 shows the UV-Visible spectra of electron irradiated and unirradiated ZnO nanoparticles. The absorption edge seen to shift towards shorter wavelength for the electron beam irradiated sample. The peak position is also seen to shift from 362 nm to 354 nm for irradiated ZnO. This occurs due to quantum size effect generated through strong interaction between the ZnO nanoparticles and high energy electrons [40, 41]. This finding shows that the irradiation affects the particle size and hence the absorption properties [40, 41].

3.3 Transmission Electron microscopy

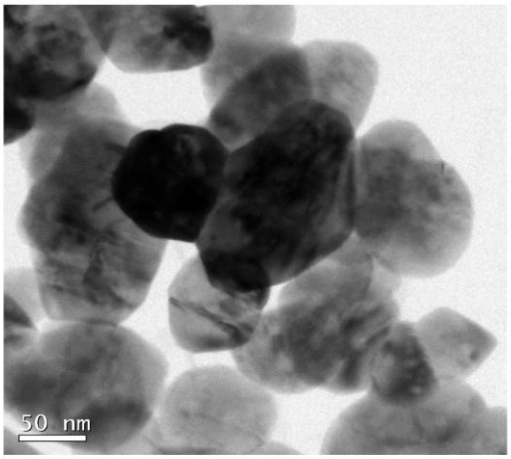

Figure 3. TEM Micrographs of ZnO NPs.

TEM images ZnO nanoparticles are shown in Fig. 3. The particles are mono disperse in nature with an average size of 40-60 nm. The nanoparticles are predominantly spherical in shape.

3.4 Surface morphology of modified electrodes

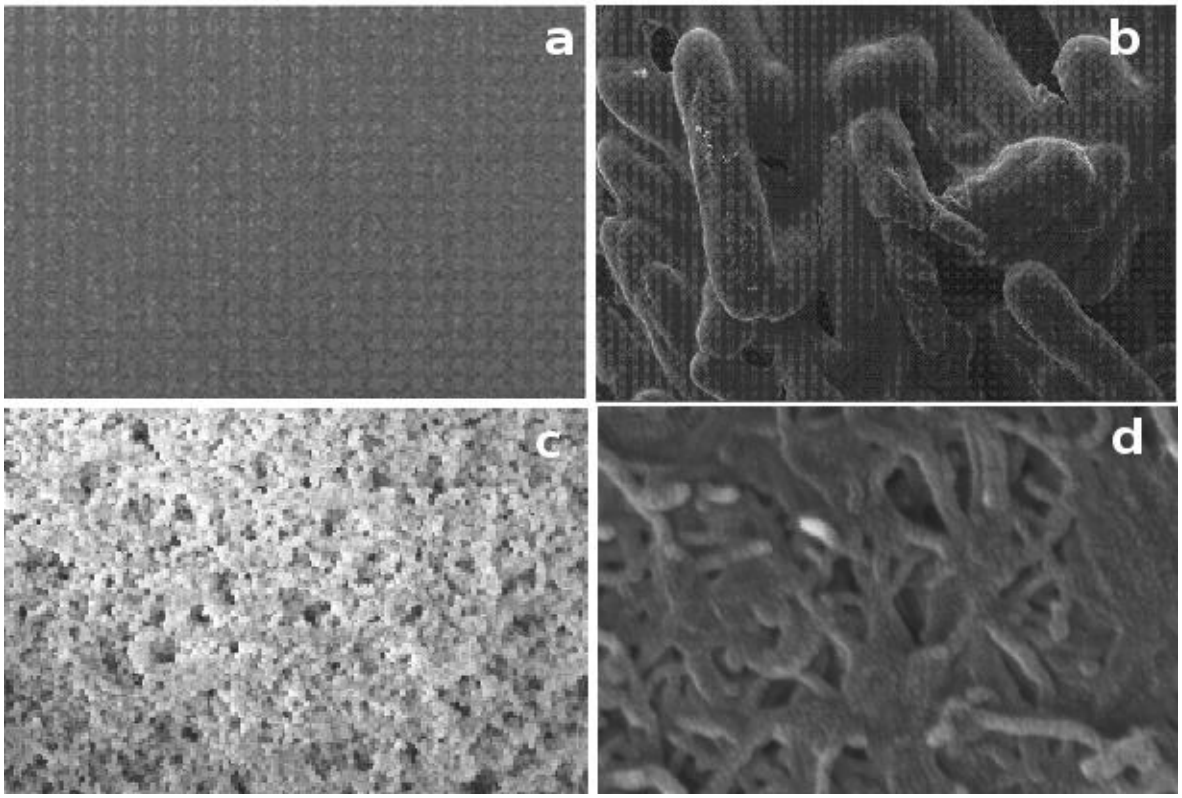

Figure 4. SEM images of (a) bare GCE (b) GCE/MWCNTs$_{OX}$ (c) GCE/ZnO & (d) GCE/ZnO/MWCNTs$_{OX}$

The SEM images of all prepared electrodes are shown in Fig. 4. The SEM images of the bare GCE (Fig. 4a), GCE/ZnO (Fig. 4b), GCE/MWCNTs$_{OX}$ (Fig. 4c) and GCE/ZnO/MWCNTs$_{OX}$ (Fig. 4d) electrodes portrayed that the electrode surfaces are effectively modified with MWCNTs$_{OX}$ and ZnO. Ii is evident from the SEM images that the bare GCE surface is uniformly covered with both ZnO and MWCNTs$_{OX}$.

3.5 Electrochemical properties of ZnO/MWCNTs$_{OX}$ electrodes.

Fig. 5 depicts the cyclic voltammograms (CVs) of GCE/ZnO, GCE/ZnO/MWCNTS$_{OX}$ (1:1), GCE/ZnO/MWCNTS$_{OX}$ (1:3) and GCE/ZnO/MWCNTS$_{OX}$ (1:5) electrodes. The capacitive behaviour of prepared electrode is evident from the rectangular type CVs. This occurs due to the synchronization of double layer and redox type supercapacitor features. It has been reported by Selvakumar et al. and Cheng et al. that as a result of the faradic reaction of ZnO redox peaks occurs in the CV, illustrating the pseudo capacitive behaviour [27]. The redox peaks (Epa, Epc1 & Epc2) were generated due to the intercalation and deintercaltion of K^+ ions into ZnO through reaction; $ZnO + K^+ + e^- \leftrightarrow ZnOK$ [26].

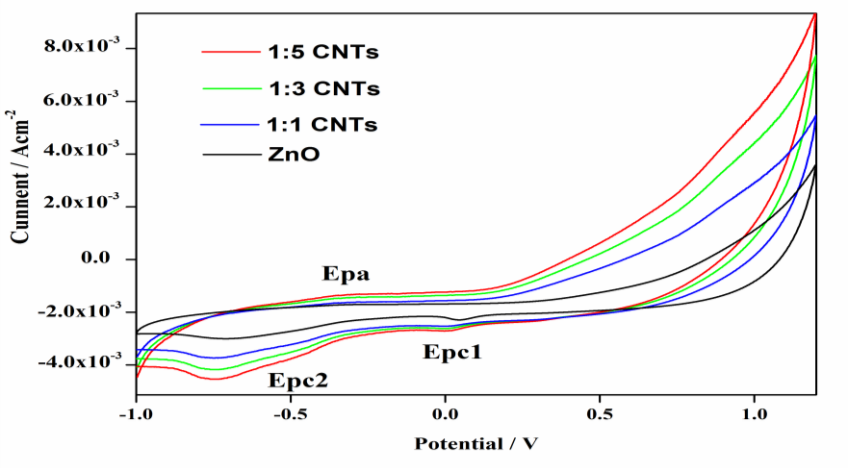

Figure 5. CVs resulted at GCE/ZnO/MWCNTs$_{OX}$ at various ratios of ZnO NPs and MWCNTs$_{OX}$. SR = 100 mV s^{-1}

Table 1. Specific capacitance values of ZnO and MWCNTs$_{OX}$ at various proportions

Ratio (w/w)	**Specific capacitance (Fg^{-1})**
1:1	340
1:3	350
1:5	**372**

The specific capacitance of the electrodes is calculated from the respective CVs using the equation, C = i/s where s is the potential sweep rate and i the average current [27]. The specific capacitance values of the various electrodes have been shown in the Table 1 and variation is shown in the fig. 6. The value of capacitance is 285 Fg^{-1} for the cell with irradiated ZnO electrode. On adding MWCNTs$_{OX}$ in different proportions to ZnO NPs modified electrodes (1:1, 1:3 & 1:5), the specific capacitance values were found to be increased. This occurs because of the combined contributions from irradiated ZnO NPs and MWCNT$_{sox}$. Overall, the 1:5 ZnO and MWCNTs$_{OX}$ cell exhibits a very high capacitance of 372 Fg^{-1} which is higher than the similar reported works. It was observed that particle size and capacitance have a direct relation. The smaller the particle size, the higher the depth of space charge region. Greater space charge regions provides better electronic conductance and thereby capacitance [42]. Herein, electron beam irradiation decreases the particle size of the ZnO NPs, which is desirable in producing high specific capacitance electrode material [43, 27]. This made us to choose electron beam irradiated ZnO NPs. Furthermore, when high energy electron beams moves through the material, it will interact with nuclei of the atom. As a result atom will excite and leave from initial position and particles energy is increased. This produces some defects because of annihilation of vacancy interstitial pairs. Creation of defects increases the electronic conductance of ZnO NPs and consequently the capacitance [40, 44].

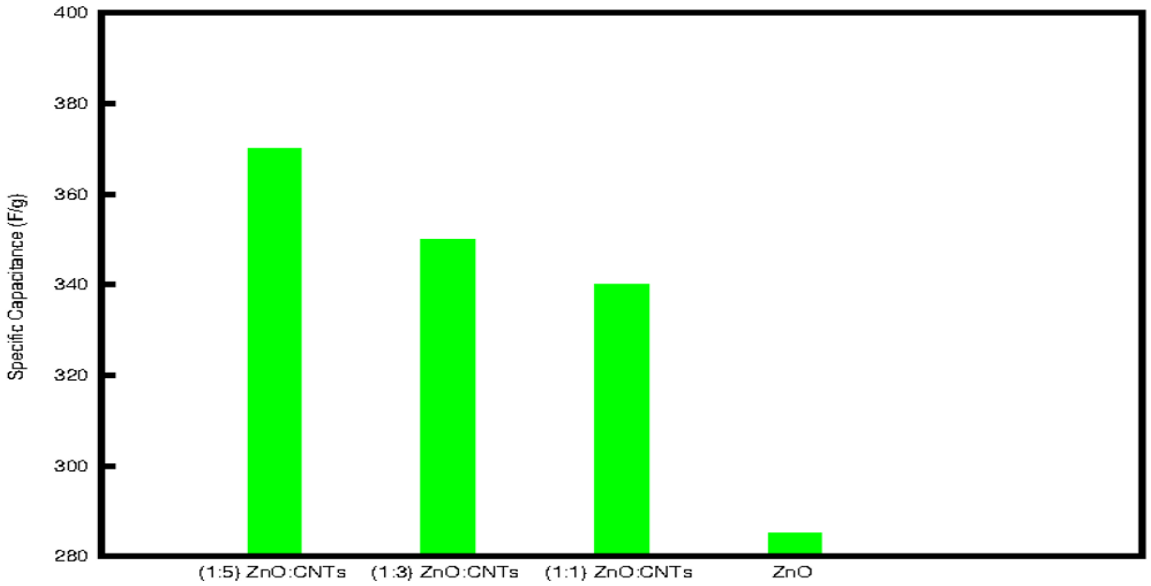

Figure 6. The specific capacitance resulted at electrodes prepared from various ratios of ZnO NPs and $MWCNTs_{OX}$.

Moreover, in the present case, the generated capacitance is also connected with double layer formed around the electrodes which can be visualized as well studied using double layer models. The proposed model is shown in scheme. 1.

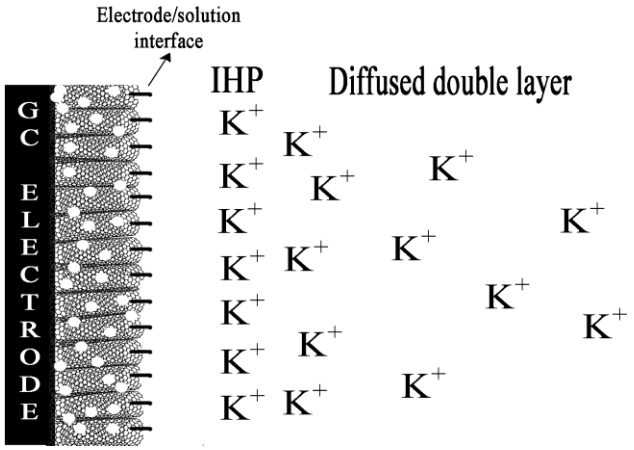

Scheme 1. The mechanism of double layer formation at GCE/ZnO/$MWCNTs_{OX}$. [IHP is Inner Helmholtz Plane]

$MWCNTs_{OX}$ carries oxygen functionalities at the ends of the tube and along the tube. These oxygen functionalities and potassium ions in bulk of solution involve in electrostatic interactions

which in turn form diffused double layer as shown in scheme 1. Electrostatic interactions between GCE/MWCNTs$_{OX}$ and potassium ions form an Inner Helmholtz Plane (IHP) at the electrode-solution interface. Moreover, a diffused double layer is formed beyond the IHP. This is attributed to the observed capacitance. Progressive addition of MWCNTs$_{OX}$ increases the oxygen functionalities at electrode surface which results in the formation of greater diffused double layer, hence greater capacitance. The combined effect of both electron beam irradiated ZnO NPs and MWC$_{NT}$sOX at the electrode surface provide a greater desired capacitance in KNO_3 solution. Desired capacitance values can be achieved by carefully controlling the amount of the MWCNTs$_{ox}$.

3.6 Characterization of electrodes using Electrochemical Impedance Spectroscopy

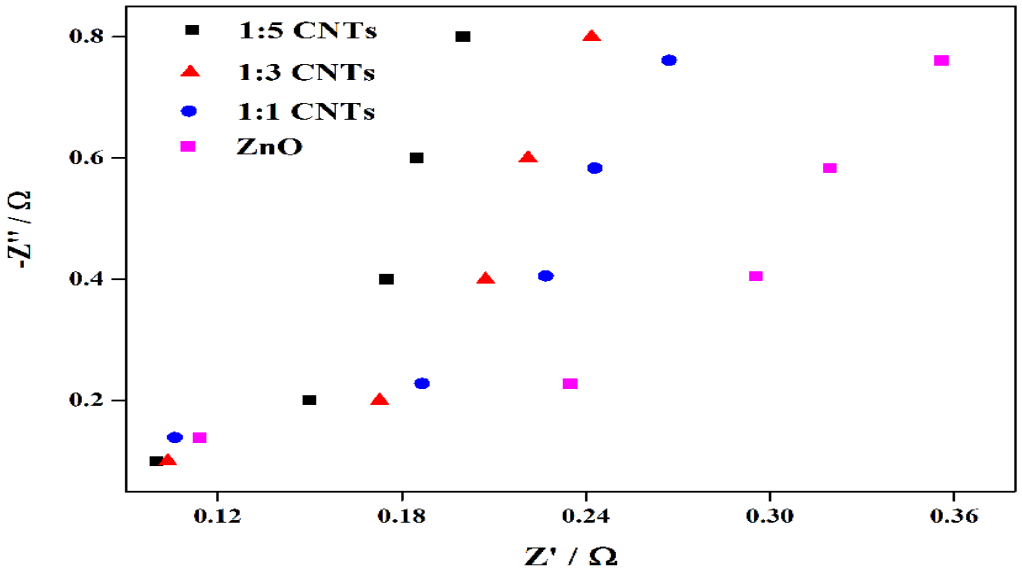

Figure 7. Nyquist plots of electrodes prepared from various ratios of ZnO NPs and MWCNTs$_{OX}$.

The EIS analysis is the principal technique to examine the fundamental behaviour of electrode materials and electrode-solution interface. EIS analyses were carried out for all the prepared electrodes. Fig. 7 shows the Nyquist plots for electrodes with three different compositions. The Nyquist plots indicate that all electrodes behave in a similar manner. The one with 1:5 ZnO NPs and MWCNTs$_{OX}$ composition exhibits the lowest charge transfer resistance and hence the greater capacitance. EIS studies further support the observations made in CV studies. Thus, the incorporation of ZnO NPs and MWCNTs$_{OX}$ can improve the charge transfer performance of GCE [27].

3.7 Comparison of performance of GCE/ZnO/MWCNTs$_{OX}$ with other electrodes

The performance of GCE/ZnO/MWCNTs$_{OX}$ was compared with other modified electrodes and the results are displayed in Table 2.

Table 2. Comparison of GCE/ZnO/MWCNTsOX with other electrode.

Electrode	Modified Electrode	Electrolyte	Specific capacitance (F/g)	Reference
Activated carbon (AC)	ZnO– (AC) 1:1 (ZnO:AC)	Na_2SO_4	76	[27]
Carbon nanotube (CNT)	CNT– ZnO 1:5 (CNT– ZnO)	PVA and PMA acid	323.9	[29]
Nano flake encapsulated carbonnanofibers (CNFs)	CNFs-ZnO 1:2 (ZnO-CNFs)	KOH	216.3	[2]
ACNF (Activated carbon nanofibers)	ZnO-ACNF Zn(20)-ACNF	KOH	178.2	[23]
GCE/ZnO/$MWCNT_{SOX}$	1:5 ZnO and $MWCNT_{SOX}$	KNO_3	372	Present work

The GCE/ZnO/$MWCNTs_{OX}$ found to have highest capacitance among other similar modified electrodes displayed in Table 1. The electron beam irradiated ZnO nanoparticles and $MWCNTs_{OX}$ forms a better electrode material having high capacitance compared to the combination of ZnO nanoparticles and activated carbon [27]. The ZnO synthesis and electrode preparation is relatively simple in the present case with better performance compared to Zhang et al. [29] The preparation of ZnO/CNF involves cumbersome procedures while the electrode preparation in the present case is simple and straight forward without any complexity [2]. Complexity is involved in the preparation of ZnO-ACNF electrode compared to the preparation of GCE/ZnO/$MWCNTs_{OX}$ having greater capacitance. The simple preparation, use of aqueous KNO_3 as electrolyte and synergetic effect of electron beam irradiated ZnO and $MWCNTs_{OX}$ make GCE/ZnO/$MWCNTs_{OX}$ supercapacitors with desired properties such as environmentally benign nature and cost effectiveness.

4. CONCLUSIONS

A supercapacitor with some prominent features has been fabricated successfully by modifying GCE with electron beam irradiated ZnO NPs and $MWCNTs_{OX}$. Herein, a ratio of 1:5 ZnO NPs and $MWCNTs_{OX}$ provide a greater specific capacitance compared to similar electrodes. The electrode with aforementioned ratio also offers the least charge transfer resistance at electrode-solution interface. Electron beam irradiated ZnO NPs enhances the performance by improving the conductance of electrode. Oxidized MWCNTs provide the larger surface area and are helpful in extending diffused double layer. The synergism of ZnO NPs and $MWCNTs_{OX}$ contributes greatly to the enhanced performance of GCE/ZnO/$MWCNTs_{OX}$. The prepared supercapacitor is environment friendly, involves

simple fabrication procedure, cycling stability and economic, which makes this electrode promising for various energy applications.

ACKNOWLEDGEMENTS

The authors thank Dr. Ganesh Sanjeev, Microtron Centre, Department of Studies in Physics, Mangalore University, Mangalagangotri, India, for electron irradiation and Joby Mathew, Assistant Professor, Department of English, St. Thomas College Pala, Kerala, India, for language editing.

References

1. B.E. Conway, *J. Electrochem. Soc.*, 138 (1991) 1539.
2. S. Shi, X. Zhuang, B. Cheng, X. Wang. *J. Mater. Chem. A*, 1 (2013) 13779–13788.
3. J.H. Jang, S.J. Han, T.W. Hyon, S.M. Oh, *J. Power Sources*, 123 (2003) 79.
4. C. Lin, X. Feng, Y.L. Yan, L.H. Lin, *Sci. Adv. Mater,* 20 (2004) 1853.
5. M. Yu, Y.M. Volfkovich, T.M. Serdyuk, *Russ. J. Electrochemistry,* 38 (2002) 935.
6. B.J. Lee, S.R. Sivakkumar, J.M. Ko, J.H. Kim, S.M. Jo, D.Y. Kim, *J. Power Sources*,168 (2007) 546.
7. C.C. Hu, K.H. Chang, C.C. Wang, *Electrochim. Acta,* 52 (2007) 4411.
8. C.D. Lokhande, T.P. Gujar, V.R. Shinde, R.S. Mane, S.H. Han, *Electrochem.Commun.,* 9 (2007) 1805.
9. A.M.P. Hussain, A. Kumar, *J. Power Sources*, 161 (2006) 1486.
10. Y. Zheng, M. Zhang, P. Gao, *Mater. Res. Bull.*, 42 (2007) 1740.
11. S.R. Sivakkumar, J.M. Ko, D.Y. Kim, B.C. Kim, G.G. Wallace, *Electrochim. Acta,* 52(2007) 7377.
12. 12. C.N.R. Rao, B. C. Satishkumar, A. Govindaraj, M. Nath, *ChemPhysChem*, 2 (2001) 78–105.
13. B.S. Sherigara, W. Kutner, F. D'Souza, *Electroanalysis*, 15 (2003) 753–772.
14. M. Pumera, *Chem. Eur. J.*, 15(2009) 4970 – 4978.
15. N. Li, J. Wang, M. Li, *Rev. Anal. Chem.,* 22 *(*2003) 19–33.
16. H. Luo, Z. Shi, N. Li, Z. Gu, Q. Zhuang, *Anal. Chem.,* 73 (2001) 915–920.
17. T. Thomas, R.J. Mascarenhas, O.J. D' Souza, S. Detriche, Z. Mekhalif, P. Martis, *Talanta,* 125 (2014) 352–360.
18. R. Kotz and M. Carlen, *Electrochim. Acta*, 45 (2000) 2483–2498.
19. S. Iijima, *Nature*, 354 (1991) 56–8.
20. T. Thomas, R.J. Mascarenhas, P. Martis, Z. Mekhalif, B.E. Kumara Swamy, *Mater. Sci. Eng. C,* 33 (2013) 3294–3302.
21. I. Dumitrescu, P.R. Unwin, Julie V. Macpherson, *Chem. Commun.*, 7(45) (2009) 6865–7052.
22. G. Lota, K. Fic, E. Frackowiak, *Energy Environ. Sci.,* 4 (2011) 1592–1605.
23. C.H. Kim, B.H Kim, *J. of Power Sources*, 274 (2015) 512-520.
24. Y. Zhang, X. Sun, L. Pan, H. Li, Z. Sun, C. Sun, B. Kang Tay, *Solid State Ion.*, 180(2009) 1525–1528.
25. D. Kalpana, K.S. Omkumar, S.S. Kumar, N.G. Renganathan, *Electrochim. Acta*, 52 (2006) 1309.
26. Y. Chen, Z. Hu, Y. Chang, H. Wang, Z. Zhang, Y. Yang, H. Wu, *J. Phys. Chem. C*, 115 (2011) 2563–2571.
27. M. Selvakumar, D. Krishna Bhat, A. Manish Aggarwal, S. Prahladh Iyer, G. Sravani, *Physica B,* 405 (2010) 2286–2289
28. L.S. Aravindaa, K.K. Nagarajab, H.S. Nagarajab, K.U. Bhat, B.R. Bhat, *Electrochim. Acta,* 95 (2013) 119.
29. Y. Zhang, X. Sun, L. Pan, H. Li, Z. Sun, C. Sun, B.K. Tay, *Solid State Ion.* 180 (2009) 1525.
30. B. Shouli, C. Liangyuan, L. Dianqing, Y. Wensheng, Y. Pengcheng, L. Zhiyong, C. Aifana, C. C. Liu. *Sens Actuator B*, 146 (2010)129–137.

31. H. Cao, Y.G. Zhao, S.T. Ho, E.W. Seelig, Q.H. Wang, R.P.H. Chang, *Phys. Rev. Lett.*,82 (1999) 2278–2281.
32. S. Stassinopoulos, R.N. Das, S.H. Anastasiadis, E.P. Giannelis, D. Anglos. *J. Opt.*,12 (2010) 024006-14 .
33. Z.L. Wang, *J. Phys.: Condens. Matter.*, 16 (2004) R829–R858.
34. C.C. Chang, J.H. Chang, *J. Mar. Sci. Technol.*, 4 (1996) 223–232.
35. S. Chu, M. Olmedo, Z. Yang, J. Kong, J. Liu, *Appl. Phys. Lett.*, 93 (2008) 181106-9 .
36. J.C. Johnson, H. Yan, R.D. Schaller, L.H. Haber, R.J. Saykally, P. Yang, *J. Phys. Chem. B*, 105 (2001) 11387–11390.
37. D. Thomas, S. Augustine, J. Prakash, *J. Optoelectronics and Biomedical Materials*, 6(4) (2014) 101 – 110.
38. Sathish Reddy, B.E. Kumara Swamy, Umesh Chandra, B.S.Sherigara, H. Jayadevappa, *Int. J. Electrochem. Sci.*, 5 (2010) 10 - 17
39. S.C Tsang, Y.K Chen, P.J.E. Harris, M.L.H Green, *Nature*, 372 *(*1994) 159–162.
40. A.V. Krasheninnikov, F. Banhart, *Nat. Mater.*, 6 (2007) 723-733.
41. K.B Sapnar, V.N Bhoraskar, S.D Dhole, *Proceedings of 2011 Particle Accelerator Conference, New York, NY, USA*, THP020 (2011) 2166-2168.
42. M. Jayalakshmi, M. Mohan Rao, Kwang-Bum Kim, *Int. J. Electrochem. Sci.*, 1 (2006) 324-333.
43. K. Siraj, Kashif Javaid, J.D. Pedarnig, M.A. Bodea, S. Naseem, *J Alloy Compd.*, 563 (2013) 280–284.
44. F. Banhart, *Rep. Prog. Phys.*, 62 (1999) 1181–1221.